

Local electric-field-induced oxidation of titanium nitride films

S. Gwo,^{a)} C.-L. Yeh, P.-F. Chen, Y.-C. Chou, and T. T. Chen

Department of Physics, National Tsing-Hua University, Hsinchu 30043, Taiwan, Republic of China

T.-S. Chao, S.-F. Hu, and T.-Y. Huang

National Nano Device Laboratory, Hsinchu 30050, Taiwan, Republic of China

(Received 7 August 1998; accepted for publication 20 December 1998)

Nanometer-scale patterning of TiN films grown on SiO₂/Si(001) has been demonstrated using the local electric-field-induced oxidation process with a conductive-probe atomic force microscope. The chemical composition of the modified TiN region was determined by micro-Auger electron spectroscopy and was found to consist of Ti, some trace amount of N, and O, suggesting the formation of titanium oxynitride in the near surface region. The dependence of the oxide height on the sample bias voltage with a fixed scanning speed shows a nonlinear trend in the high electric field regime, indicating that the growth kinetics might be significantly different from previous studies using other film materials. © 1999 American Institute of Physics. [S0003-6951(99)03208-8]

Proximal probe induced anodic oxidation has become a promising new nanofabrication process that is capable of producing surface oxide patterns on the nanometer length scale. At present, atomic force microscope and scanning tunneling microscope (AFM/STM) based anodization of Si¹⁻⁶ and metal films (Ti,⁶⁻⁹ Nb,^{10,11} Al,¹² etc.) has been reported by a number of research groups. Furthermore, several prototypes of devices based on quantum size effects have been demonstrated.^{8,11,12} The local field-induced oxidation (FIO) process is similar to conventional electrochemical anodization except that an AFM/STM tip is used as the cathode and water from the ambient humidity is used as the electrolyte. Due to the ambient nature of this process, a metallurgically stable and chemically resistant film is preferred as the base material.

Titanium nitride belongs to the family of refractory transition metal nitrides and exhibits characteristics of both covalent compounds such as high melting points, thermodynamic stability, extreme hardness, and of metals such as good thermal and electrical conductivity. It has been extensively used in metallization schemes for silicon ultra large-scale integrated circuits as the material for diffusion barriers, rectifying and ohmic contacts, and gate electrodes in field-effect transistors. Also, it has been used widely as tribological coatings in cutting tools and by coating industries. The resistivities of TiN films can be varied greatly by oxidation. For example, oxidation of TiN to TiO₂ is accompanied by a resistivity increase of many orders of magnitude (resistivities of TiO₂ films in the order of 10⁶ Ω cm and resistivities of TiN films ≈ 25–800 × 10⁻⁶ Ω cm). This material property offers us a possibility of obtaining a lateral barrier layer by selective oxidation from a single layer of TiN. Additionally, oxidized TiN films can also be used to form antireflection coatings. Therefore, it is an attractive candidate material for nanometer-scale lithographic applications using the scanned local probe approach in the ambient environment.

TiN thin films of ≈ 5 nm thickness were deposited by reactive sputtering technique from a pure Ti target onto

Si(001) wafers covered with 100 nm of thermal SiO₂ in an atmosphere of a 1:1 Ar/N₂ gas mixture. The gas flow rate (30/30 sccm) of the sputtering gas was adjusted to give a working pressure of 3.5–4 mTorr. During deposition, the sputtering power was 0.5 kW and the deposition rate was 0.1 nm/s. The average surface roughness of the deposited films as measured by AFM is around 0.2–0.3 nm. Local oxidation was performed in air using boron doped p⁺-Si cantilevers (10 nm average tip radius) and a commercial AFM/STM microscope (CP type, Park Scientific Instruments, CA). The average force constant and resonance frequency of the cantilevers used (UltraleversTM) are about 0.26 N/m and 40 kHz, respectively. The relative humidity during experiments was around 65%. When performing local oxidation, a positive voltage to the sample with respect to the tip was applied at pre-selected lines (so-called “vector” mode) while scanning the sample surface.

Shown in Fig. 1(a) is an example of modified film topography, demonstrating the possibility of performing nanometer-scale lithography using the local FIO process on TiN films. In the protruded pattern (two vertically aligned grids) a sample bias of +8 V was applied during the pattern scanning (the writing speed was 0.25 μm/s) while normally the sample bias was grounded. In Fig. 1(b), we can find the cross-sectional line height is ≈ 3.5 nm along the x direction and ≈ 4.5 nm along the y direction. And the cross-sectional linewidth [full width at half maximum (FWHM)] is ≈ 60 nm along the x direction and ≈ 30 nm along the y direction. Since the lithographic conditions were identical except scanning along two orthogonal directions, we believe that the observed anisotropic cross-sectional profiling is a consequence of an asymmetric tip shape. The protruded feature is consistent with the fact that the oxidation of TiN is accompanied by a volume expansion. For example, the molar volume from TiN to TiO₂ increases ≈ 60%. Also, it can be seen from the AFM image that the FIO induced feature is highly uniform and the process itself is very reproducible as long as a stable tip shape/size and a constant operating environment

^{a)}Electronic mail: gwo@phys.nthu.edu.tw

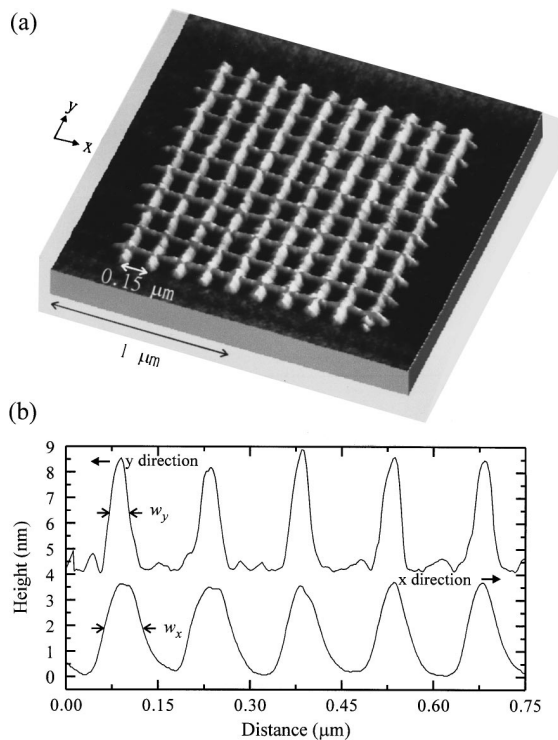


FIG. 1. (a) AFM image of two vertically aligned grids of oxidized lines on TiN. (b) Cross-sectional line profiles along two grid directions. In this plot, the oxide line height and the oxide linewidth (FWHM) along the x and y directions are 3.5, 60 nm and 4.5, 30 nm, respectively. The distance between lines is 150 nm. Local oxidation conditions: tip scanning speed 0.25 $\mu\text{m/s}$, sample bias +8 V, relative humidity 65%.

are maintained during the lithography procedure. At present, the optimal linewidth, depending on the tip size, applied sample bias, scanning speed, and environment humidity, etc., that can be obtained by this process is around 10–20 nm.

In order to investigate the chemical composition of the locally oxidized structure, scanning Auger microscopy (SAM) and Auger electron spectroscopy (AES) analyses were conducted on a large $5 \times 5 \mu\text{m}^2$ oxidized area (5–6 nm oxide height) using a PHI model 670 Auger Nanoprobe™ system with Schottky field emission electron source. The Auger spectra taken from the modified and unmodified regions are shown in Figs. 2(a) and 2(b). In both spectra we can see the clear emission peak of O $KL_{23}L_{23}$ Auger electrons having kinetic energy of ≈ 502 eV. However, the oxygen to titanium intensity ratio is much greater in the modified region than that in the unmodified region. This is consistent with the previous suggestion that an enhanced incorporation of oxygen occurred in the FIO process and the much weaker oxygen signal in the unmodified region originated from the native oxide.¹³ The carbon signal observed in these spectra may be due to slight carbon contamination since no sputter cleaning procedure was employed. Quantitative chemical analysis of titanium nitrides by AES is complicated by the fact that the main $KL_{23}L_{23}$ Auger electron emission from nitrogen occurs at an energy that overlaps the $L_3M_{23}M_{23}$ transition from titanium at ≈ 385 eV.^{14,15} Since there are no N Auger transitions above 400 eV, the Auger emission at ≈ 418 eV arises solely from the Ti $L_3M_{23}M_{45}$ transition. Therefore, this transition can represent the Ti intensity and chemical fingerprinting for titanium nitride. Several quanti-

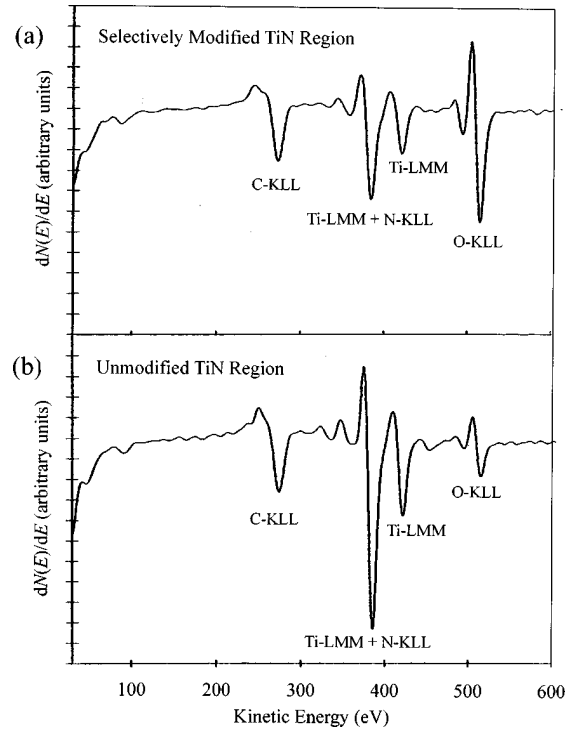


FIG. 2. Micro-Auger analysis of a thin TiN film for (a) the oxidized region ($5 \times 5 \mu\text{m}^2$) by the local electric-field-induced oxidation process and (b) the unmodified region of the film. Clear enhanced peak of oxygen is detected in the locally oxidized region.

fication schemes have been proposed to derive the N component from the overlapping transitions at ≈ 385 eV using the Ti Auger emission peak height at ≈ 418 eV.^{14,15} The analysis result using the approach proposed by Dawson and Tzatzov¹⁵ indicates that our TiN films are nearly stoichiometric.

Interestingly, the Auger spectrum result on the selectively oxidized TiN surface in our experiment closely resembles the published data of Matsumoto *et al.*¹³ on a selectively oxidized Ti surface, indicating a very similar chemical composition on both surfaces. However, the detailed quantitative analysis reveals that the peak height ratio between the ≈ 385 and the ≈ 418 eV peak is greater for Auger spectrum taken from the FIO modified TiN than that from the FIO modified Ti ($\approx 15\%$ greater). It implies that some trace amount of nitrogen still remains on the TiN surface after the FIO process. Since Auger spectroscopy is a surface sensitive technique (escape depth ≤ 1 nm at 300–500 eV electron kinetic energies), it is very difficult to derive the exact chemical nature of the underlying oxide layer from the Auger data alone. For the case of thermally oxidized TiN in dry O_2 , the oxidation reaction: $\text{TiN} + \text{O}_2 \rightarrow \text{TiO}_2 + (1/2)\text{N}_2$ has been found thermodynamically favorable and the rutile form of TiO_2 is the main product.¹⁶ On the other hand, Montero *et al.*,¹⁷ using Rutherford backscattering spectrometry and nuclear reaction analysis techniques, showed that the anodically oxidized TiN films contains an oxygen-enriched TiN_xO_y transition layer formed between the underlying TiN and the top TiO_2 layer. Their result suggests that outdiffusion of N atoms and indiffusion of replacing oxidant specie probably occur during the formation of oxide by the anodization process. And, the concentration gradients of N and O atoms in

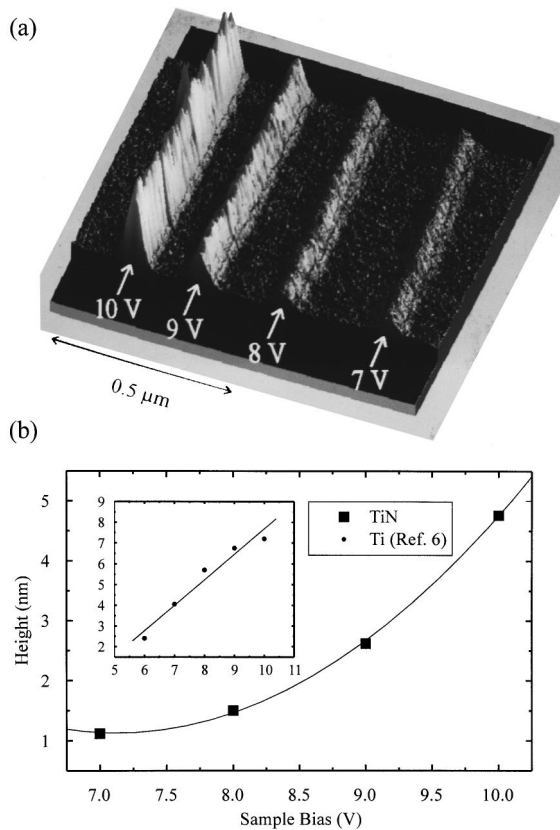


FIG. 3. (a) Four oxidized lines formed on the titanium nitride film by the AFM conductive probe induced local oxidation process at different sample biases (+10, +9, +8, +7 V, respectively). The tip scanning speed during line writing was fixed at $0.1 \mu\text{m/s}$ and relative humidity was 65%. (b) The averaged oxide height vs sample bias plot. Inset in (b) shows data from Ref. 6.

the grown oxide film are most likely caused by the overall transport reaction.

To understand the FIO kinetics on TiN, we have also performed oxide line writing with varied sample biases. AFM image shown in Fig. 3(a) is the dependence of the oxide height (H) versus the sample bias voltage (V_s) with a fixed writing speed ($0.1 \mu\text{m/s}$). In Fig. 3(b), the averaged cross-sectional oxide height (averaged along the oxide lines) is plotted versus sample bias. In the range of high sample biases used (+7–+10 V), the fitted line shows a nonlinear dependence of the oxide height on the magnitude of the applied sample bias. The linear relationship between H and V_s has been reported for the FIO process on various film materials. For comparison, results of previous FIO study on thin Ti films⁶ are plotted in the inset of Fig. 3(b), where a clear linear relationship can be seen (except at the high bias end, where the saturation of the oxide height occurs). Our kinetic study results suggest that a significantly different oxidation kinetics exists for the TiN film case in the high electric field regime, mainly resulted from the graded chemical composition when forming oxide layer on binary TiN compound films by the FIO process.

The most cited kinetic model to describe the FIO process

for the case of growing very thin films was proposed by N. Cabrera and N. F. Mott.^{18–20} In this model, the strong electric field resulted from the applied bias across the film enhances the injection of metallic cations from the substrate or the injection of oxidant anions from the oxide surface into the oxide film. Here it is worth noting that the electric field E is assumed to be uniform ($= V_s/H$) throughout the thin film and the growth rate is limited by the decay of the electric field E with increasing height H . On the other hand, the oxidation layer of TiN produced by anodization contains a graded TiN_xO_y transition layer. As a consequence, the electric field is not uniform across the oxide layer. In addition, the ambient FIO process of TiN involves complicated bi-directional transport due to incorporation of O and loss of N across the transition and oxide layers. Detailed modeling is now under way to explain the growth kinetics observed in our FIO experiments on TiN films.

In summary, nanometer-scale surface oxide patterning of TiN metallic films has been demonstrated for the first time using the AFM local electric-field-induced oxidation process. The chemical composition of the selectively oxidized TiN area was determined by micro-Auger analysis. We suggest a formation of TiN_xO_y graded oxide layer in the near surface region.

This work was supported partly by the National Science Council (Contract Nos. NSC 87-2112-M-007-003 and NSC 88-2112-M-007-002), Taiwan, Republic of China.

¹J. A. Dagata, J. Schneir, H. H. Harary, C. J. Evans, M. T. Postek, and J. Bennet, *Appl. Phys. Lett.* **56**, 2001 (1990).

²L. A. Nagahara, T. Thundat, and S. M. Lindsay, *Appl. Phys. Lett.* **57**, 270 (1990).

³T. Teuschler, K. Mahr, S. Miyazaki, M. Hundhausen, and L. Ley, *Appl. Phys. Lett.* **67**, 3144 (1995).

⁴Ph. Avouris, T. Hertel, and R. Martel, *Appl. Phys. Lett.* **71**, 285 (1997).

⁵R. García, M. Calleja, and F. Pérez-Murano, *Appl. Phys. Lett.* **72**, 2295 (1998).

⁶E. Dubois and P. A. Fontaine, *Extended Abstracts in Solid State Devices and Materials Conference* (Hamamatsu, Japan, 1997), p. 474.

⁷H. Sugimura, T. Uchida, N. Kitamura, and H. Masuhara, *Appl. Phys. Lett.* **63**, 1288 (1993).

⁸K. Matsumoto, M. Ishii, K. Segawa, and Y. Oka, *Appl. Phys. Lett.* **68**, 34 (1996).

⁹B. Irmer, M. Kehrle, H. Lorenz, and J. P. Kotthaus, *Appl. Phys. Lett.* **71**, 1733 (1997).

¹⁰J. Shirakashi, M. Ishii, K. Matsumoto, N. Miura, and M. Konagai, *Jpn. J. Appl. Phys., Part 2* **35**, L1524 (1996).

¹¹J. Shirakashi, K. Matsumoto, N. Miura, and M. Konagai, *Jpn. J. Appl. Phys., Part 2* **36**, L1257 (1997).

¹²E. S. Snow, D. Park, and P. M. Campbell, *Appl. Phys. Lett.* **69**, 269 (1996).

¹³K. Matsumoto, S. Takahashi, M. Ishii, M. Hoshi, A. Kurokawa, S. Ichimura, and A. Ando, *Jpn. J. Appl. Phys., Part 1* **34**, 1387 (1995).

¹⁴J.-E. Sundgren, B.-O. Johansson, and S.-E. Karlsson, *Surf. Sci.* **128**, 265 (1983).

¹⁵P. T. Dawson and K. K. Tzatzov, *Surf. Sci.* **149**, 105 (1985).

¹⁶M. Wittmer, J. Noser, and H. Melchior, *J. Appl. Phys.* **52**, 6659 (1981).

¹⁷I. Montero, C. Jiménez, and J. Perrière, *Surf. Sci.* **251/252**, 1038 (1991).

¹⁸N. Cabrera and N. F. Mott, *Rep. Prog. Phys.* **12**, 163 (1949).

¹⁹A. Atkinson, *Rev. Mod. Phys.* **57**, 437 (1985).

²⁰D. Stiévenard, P. A. Fontaine, and E. Dubois, *Appl. Phys. Lett.* **70**, 3272 (1997).